UCRL-JC-126647
PREPRINT

Accurate Atomistic Simulations of the Peierls Barrier and Kink-Pair Formation Energy for <111> Screw Dislocations in bcc-Mo

W. Xu
J. Moriarty

This paper was prepared for submittal to the
American Physical Society Meeting
Kansas City, MO
March 17-21, 1997

May 1997

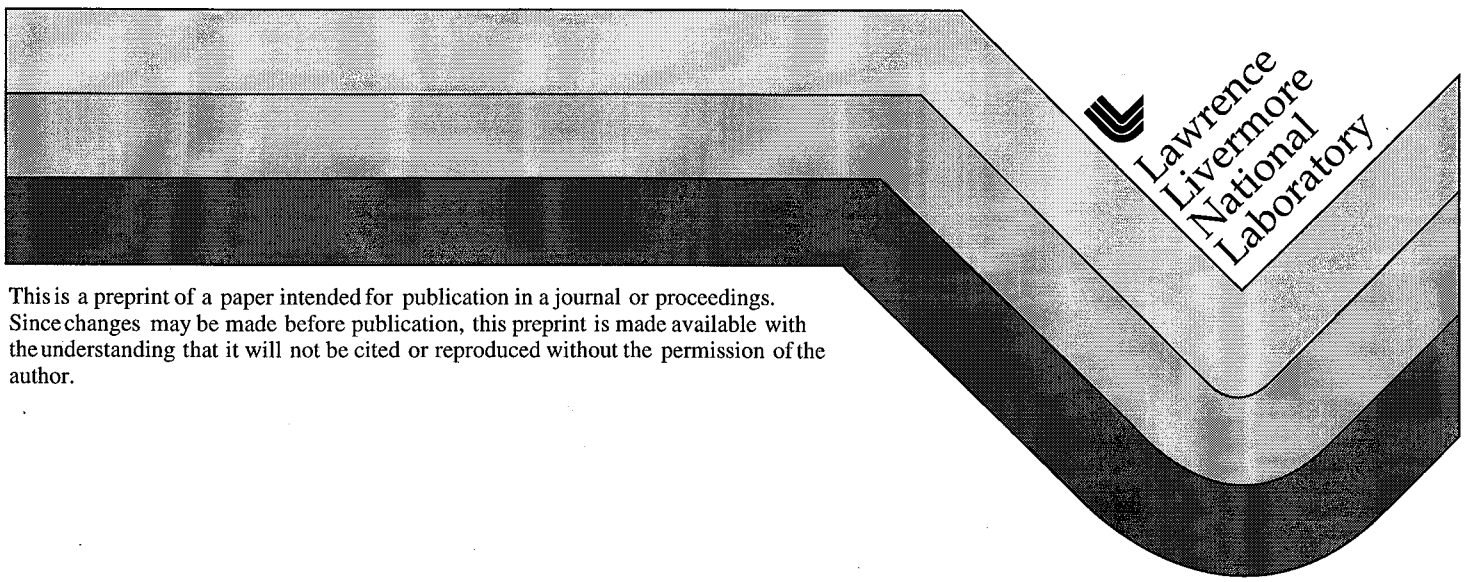

Accurate atomistic simulations of the Peierls barrier and kink-pair formation energy for <111> screw dislocations in bcc Mo

Wei Xu and John A. Moriarty

Lawrence Livermore National Laboratory, University of California, Livermore, California 94551

(May 23, 1997)

Abstract

Using multi-ion MGPT interatomic potentials derived from first-principles generalized pseudopotential theory, we have performed accurate atomistic simulations on the energetics of dislocation motion in the bcc transition metal Mo. Our calculated results include the (110) and (211) generalized stacking fault (γ) energy surfaces, the Peierls stress required to move an ideal straight <111> screw dislocation, and the kink-pair formation energy for nonstraight screw dislocations. Many-body angular forces, which are accounted for in the present theory through explicit three- and four-ion potentials, are quantitatively important to such properties for the bcc transition metals. This is demonstrated explicitly through the calculated γ surfaces, which are found to be 10-50% higher in energy than those obtained with pure radial-force models. The Peierls stress for an applied <111>/{112} shear is computed to be about 0.025μ, where μ is the bulk shear modulus. For zero applied stress, stable kink pairs are predicted to form for kink lengths greater than $4b$, where b is the magnitude of the Burgers vector. For long kinks greater than $15b$, the calculated asymptotic value of the kink-pair formation energy is 2.0 eV.

61.72.Bb,61.72.Lk,61.82.Bg,62.20.Fe

I. INTRODUCTION

In bcc transition metals, the low-temperature and high-strain-rate plastic deformation properties differ dramatically from those of the fcc metals. In particular, there is a rapid increase of flow stress with decreasing temperature and a breakdown of the Schmid law of critical resolved shear stress (for reviews, see Refs. [1] and [2]). Experimental observations suggest that screw dislocations in bcc transition metals are much less mobile than edge dislocations and, consequently, screw-dislocation behavior is the limiting factor which controls both low-temperature and high-strain-rate plasticity. It is also widely believed that a double-kink Peierls-barrier mechanism is responsible for the actual mobility of the screw dislocations. To understand the underlying mechanisms in detail, however, it is necessary to carry out accurate atomistic simulations on the structure and energetics of single dislocations, as well as on dislocation-dislocation interactions. Moreover, an accurate atomistic description of dislocation energetics can be used as input into larger length scale theories and simulations in the multiscale modeling of plastic flow and other mechanical properties. For example, the activation energy for the double-kink motion of <111> screw dislocations has been identified as a key parameter for the 3D dislocation dynamics simulation of microstructural evolution in bcc metals [3].

Accurate atomistic simulations of deformation and defect energetics in bcc transition metals require a quantum-mechanical treatment of the strong angular forces present in these materials, which arise from multi-ion d-state interactions [4–7]. Moriarty [5] has derived appropriate quantum-based multi-ion interatomic potentials for transition metals from first-principles generalized pseudopotential theory (GPT). For atomistic simulations on the bcc metals, a simplified model GPT (MGPT) has been developed using canonical d bands. This produces entirely analytic three- and four-ion potentials which are both computationally efficient and physically robust [6–8]. In the case of molybdenum (Mo), MGPT potentials have been successfully applied to the cohesive, structural, elastic, vibrational, thermal, and melting properties of the bulk metal [7]. In a recent paper [8], we have also used the same

potentials to calculate a wide variety of deformation and defect properties of bcc Mo with considerable success, including the equilibrium structure of the <111> screw dislocation core. In the present work, we have further investigated the energetics and motion of these screw dislocations on the primary {110} and {112} slip planes in the bcc lattice. Specifically, we report here on calculations of the generalized stacking fault (γ) energy surfaces and on the Peierls stress and related energetic barriers associated with the motion of ideal straight <111> screw dislocations in bcc Mo. We also report on corresponding calculations of the kink-pair formation energy for these dislocations as a function of kink length.

This paper is organized as follows. In Sec. II, we briefly review the MGPT interatomic potentials for Mo and discuss the general simulation method used in this work to treat generalized stacking faults and dislocations. Our detailed calculations of the γ surfaces for the (110) and (211) slip planes in Mo are presented in Sec. III. The calculation of the ideal Peierls stress and related energy barriers for <111> screw dislocation motion is then discussed in Sec. IV. In Sec. V we describe our initial simulations of kink-pair formation on these dislocations. Finally, our conclusions are given in Sec. VI.

II. THEORETICAL APPROACH

The angular-force, multi-ion MGPT interatomic potentials used in our atomistic simulations are based on first-principles generalized pseudopotential theory [5]. Complete details of the MGPT formalism as it applies here to Mo are discussed in Refs. [6–8], and the Mo potentials themselves can be obtained by the interested reader as described in Ref. [9]. Briefly, the first-principles GPT provides a rigorous real-space expansion of the total-energy functional of a bulk transition metal in the form

$$E_{tot}(\mathbf{R}_1...\mathbf{R}_N) = NE_{vol}(\Omega) + \frac{1}{2}\sum_{i,j}{}' v_2(ij) + \frac{1}{6}\sum_{i,j,k}{}' v_3(ijk) + \frac{1}{24}\sum_{i,j,k,l}{}' v_4(ijkl) \ , \qquad (1)$$

where $\mathbf{R}_1...\mathbf{R}_N$ denotes the positions on the N ions in the metal, Ω is the atomic volume, and the prime on each sum over ion positions excludes all self-interaction terms where two

indices are equal. The leading volume term in this expansion, E_{vol}, as well as the two-, three-, and four-ion interatomic potentials, v_2, v_3 and v_4, are volume dependent, but *structure independent* quantities and thus *transferable* to all bulk ion configurations. In the MGPT, the potentials v_2, v_3, and v_4 are systematically approximated by introducing canonical d bands and other simplifications to achieve short-ranged, analytic forms. The radial-force, two-ion pair potential v_2 is obtained as a sum of simple-metal sp, hard-core overlap, and tight-binding-like d-state contributions. The angular-force three- and four-ion potentials, v_3 and v_4, are obtained as the appropriate multi-ion generalizations of the d-state component to v_2. The potential v_3 is a three-dimensional function of the separation distances linking three ions, while the potential v_4 is a six-dimensional function of the six separation distances linking four ions. These latter potentials have exact analytic representations which are given in Ref. [6]. In the MGPT, one compensates for the additional approximations introduced to achieve analytic potentials by parameterizing the five coefficients of the d-state contributions to v_2, v_3, and v_4. For the present Mo potentials at the observed equilibrium volume, one of the five parameters has been obtained from first-principle considerations while the other four have been fit to bulk experimental elastic constants and the vacancy formation energy, as described in Ref. [7]. All remaining quantities have been calculated from first-principles.

The general simulation method used to implement the MGPT potentials in the present work is based on total-energy minimization at zero temperature and utilizes a rectangular slab-shaped computational cell, whose cross section is depicted in Fig. 1. Here the z axis is chosen perpendicular to the slab, so the cross section is in the xy plane. The cell is divided into an atomistic region, denoted as I in the figure, and a boundary-layer region, denoted as II. The atomic positions in region II are determined by imposing either fixed or periodic boundary conditions in the x and y directions. Fixed or periodic boundary conditions are also applied along the z direction perpendicular to the slab. In the atomistic region, all atoms are allowed to fully relax via a standard conjugate-gradient technique, subject to the boundary conditions imposed in region II and along the z direction. For a given set of boundary conditions, the size of region I and/or the thickness of the slab can be increased

until convergence is reached. The thickness of region II, on the other hand, is fixed by the effective range of the interatomic potentials. For the present Mo potentials, this thickness is $2a$, where a is the bulk bcc lattice constant.

Within this general scheme, a stacking fault in the otherwise perfect bcc lattice can be modeled by choosing a thick, narrow slab with periodic boundary conditions applied in the x and y directions and fixed boundary conditions applied in the z direction perpendicular to the fault plane. Specifically, the generalized stacking fault defined by Vitek [2] is created by rigidly displacing the top half of such a slab with respect to the bottom half, allowing relaxation only in the z direction. The ideal <111> screw dislocation, on the other hand, is modeled by a thin, wide slab with the z axis parallel or anti-parallel to the Burgers vector $\mathbf{b}$, with the dislocation core centered in the xy plane of the computational cell. The x and y axes are here chosen along <112> and <110> directions, respectively. Periodic boundary conditions are applied in the z direction, in order to simulate an infinite straight screw dislocation, with a slab thickness of $2b = \sqrt{3}a$. In the x and y directions, we use fixed boundary conditions with the positions of the atoms in region II established by linear anisotropic elasticity theory [10]. The dislocation core, whose radial extent is on the order of $2b$, is contained entirely within region I in all cases. This scheme can be readily generalized to accomodate an applied stress on the dislocation core and/or a double kink along the dislocation line. An applied stress is simulated by imposing a corresponding homogeneous shear strain, as given by linear elasticity, on the equilibrium dislocation core configuration. That is, the atomic positions in region II are adjusted according to the prescribed strain, while the atoms in region I are allowed to relax to new equilibrium positions. A double kink is treated by using a thick slab to appropriately reduce the periodicity in the z direction. In this case the slab thickness must be large compared to the kink length R_k.

Constrained moves of the straight screw dislocation in the xy plane are also possible within our computational scheme. These are accomplished with a reaction coordinate method in this work and are useful to estimate the energy barrier to dislocation motion along prescribed paths. In this method, one identifies a single atomic row (parallel to the

dislocation line) which has the largest displacements resulting from the movement of the dislocation core from one equilibrium site to a neighboring site. We then march this atomic row from its initial position to its final position. During the migration process, we allow this atomic row to relax in the xy plane. At the same time, all other atoms in region I are fully relaxed, while the atoms in region II remained fixed.

III. GENERALIZED STACKING FAULT ENERGY SURFACES

The stability of stacking faults on the slip planes of a crystal are intimately connected to the mobility of dislocations on these planes. In close-packed structures, both stable and unstable stacking faults are produced by the relative translation of two parts of a crystal through a vector $\mathbf{f}$ which is a rational fraction of a lattice vector. The fault is introduced by cutting a crystal block along the fault plane and shifting the upper part with respect to the lower part by a vector $\mathbf{f} = x\mathbf{a_1} + y\mathbf{a_2}$, where $\mathbf{a_1}$ and $\mathbf{a_2}$ are two lattice vectors which characterise the fault plane and $0 < \{x, y\} < 1$. A generalized stacking fault (γ) energy surface is generated by varying x and y over this entire domain for a given fault plane. In the present work, we have calculated γ surfaces for the (110) and (211) slip planes in bcc Mo. To obtain adequate convergence, a computational cell with a slab thickness of about $80a$ has been used. As indicated above, in the perpendicular x and y directions, we have applied periodic boundary conditions to mimic an infinite fault plane. The whole structure was then allowed to relax perpendicular to the fault plane.

Our calculated (110) and (211) γ surfaces for bcc Mo are illustrated in Fig. 2. The lattice vectors $\mathbf{a_1}$ and $\mathbf{a_2}$ for these two cases are along $[1\bar{1}0]$ and [001] for the (110) surface and along $[0\bar{1}1]$ and $[\bar{1}11]$ for the (211) surface, respectively. Neither γ surface shows any non-bcc local minima, indicating that no stable stacking faults with single-layer width are predicted to exist for the {110} and {112} slip planes. On the (110) surface, unstable stacking faults (saddle points) are readily seen along the diagonal ($x = y$) directions. The (211) γ surface also displays the so-called twinning–anti-twinning (t-a) asymmetry along the $[\bar{1}11]$

direction, which implies non-Schmid slip behavior on this plane. *Qualitatively*, all of these features agree with those obtained from previous atomistic studies [2] using radial-force pair potentials and from more recent studies [11] using many-body, but still radial-force, Finnis-Sinclair potentials [12]. *Quantitatively*, however, there are significant differences between the γ surfaces calculated from such potentials and from the present angular-force MGPT potentials. Specifically, the MGPT potentials yield consistently higher energies for both γ surfaces in Mo. Our maximum calculated energies on the (110) and (211) surfaces are 201 meV/$\AA^2$ and 251 meV/$\AA^2$, respectively. These energies are 45% higher for the (110) surface and 14% higher for the (211) surface than obtained using the Finnis-Sinclair potentials.

IV. PEIERLS STRESS AND ENERGY BARRIERS FOR <111> SCREW DISLOCATIONS

The possible core configurations of a <111> screw dislocation in bcc Mo have been carefully studied with the MGPT potentials and the results reported in a previous paper [8]. Two mechanically stable configurations were found, the so-called "easy-" and "hard-"core dislocations. These two configurations can be obtained either with (i) a common geometrical center and Burgers vectors in opposite directions or with (ii) a common Burgers vector and geometrical centers displaced, as described below. The standard differential-displacement-map representations [2] of these configurations are displayed in Fig. 3. Both configurations are nonplanar in character and possess three-fold symmetry. The "easy" core is the stable ground state and is spread out in three <112> directions on {110} planes. Because there are six possible <112> directions here, the "easy" core can have either of two orientations and is thus doubly degenerate. The higher-energy and higher-symmetry "hard" core is more compact without any directional spreadout. This configuration is nondegenerate with a calculated formation energy that is 0.24 eV/b higher than that of the stable "easy" core.

The minimum or Peierls stress to move a rigid screw dislocation in the bcc lattice depends strongly on the orientation of the applied stress [13]. As a step towards determining

the full orientation dependence of the Peierls stress in Mo, we have examined the application of pure shear or glide stresses on the relaxed "easy"-core dislocation. As indicated above, such stresses have been imposed by introducing a homogeneous shear strain over the entire simulation cell. Then, keeping the atoms in the boundary-layer region II fixed, the atomic positions of the inner region I were relaxed. For each applied stress, the resultant configuration was examined for any change in the location of the core. If the core was displaced from its unstressed location, the dislocation was taken to have moved and the applied external stress was taken as an upper limit to the Peierls stress. Using a binary search, the minimum stress to initiate motion was thereby determined for each orientation considered.

In general, only two pure shear stresses, σ_{zx} and σ_{zy}, can generate a nonzero glide force (Peach-Koehler force) on the <111> screw dislocation. These are stresses oriented along the <111> direction on {112} and {110} planes, respectively. For a $15a \times 15a$ region-I computational cell, we have found corresponding minimum shear stresses to move the <111> screw dislocation of about 0.03μ and 0.04μ, where μ is the shear modulus $(C_{11}-C_{12}+C_{44})/3$ with a value of 1.376 Mbar for bcc Mo. In both cases the dislocation moves on a primary {110} slip plane. For the case of the σ_{zx} stress, we have also examined the dependence of the result on the simulation cell size. The Peierls stress was found to decrease 20% when the cell size was increased from $15a \times 15a$ to $20a \times 20a$. Further enlarging the cell size to $25a \times 25a$, the Peierls stress changed only a few percent, however. For the $25a \times 25a$ cell, the calculated Peierls stress attains an approximately converged value of 0.025μ.

Using the reaction coordinate technique discussed in Sec. II, we have also calculated the energy barriers for constrained moves of an "easy" core on the {110} and {112} slip planes. In Fig. 4, we have labeled the possible equilibrium sites for the dislocation core as 1, 2, 3, or 4. For a given orientation of the Burgers vector **b**, sites 1 and 4 are stable "easy"-core sites and 2 and 3 are metastable "hard"-core sites. For movement in a <112> direction on a {110} plane, we envisage a sequence of nearest-neighbor moves or "jumps" between "easy" and "hard" sites such as $1 \rightarrow 2 \rightarrow 4$. As shown in the figure, the height of the energy barrier for moves from $1 \rightarrow 2$ or $4 \rightarrow 2$ is 0.26 eV/b, while only a very shallow barrier of 0.02 eV/b

must be overcome to move from $2 \rightarrow 4$ or $2 \rightarrow 1$. Similarly, moving in a <110> direction on a $\{112\}$ plane involves a path like $2 \rightarrow 1 \rightarrow 3$. The barrier to move from $2 \rightarrow 1$ is still 0.02 eV/b. However, one has to overcome a very much higher barrier of 0.90 eV/b to move from $1 \rightarrow 3$ on the $\{112\}$ plane. This shows that the core prefers to move on the $\{110\}$ plane in bcc Mo. Furthermore, the asymmetrical energy barriers on the $\{112\}$ plane will result in different slopes and hence different stresses depending on the path. This confirms that the shear stress to move a screw dislocation on a $\{112\}$ plane will depend on the direction of the slip, as is implied by the twinning–anti-twinning asymmetry of the γ surface.

V. KINK-PAIR FORMATION ON <111> SCREW DISLOCATIONS

We have also considered kink-pair formation on a <111> screw dislocation in bcc Mo with zero applied stress. To construct a kink pair, we first generated a screw dislocation (d_1) with its core located at site 1, as shown in Fig. 5. Next, the central part of this dislocation was replaced by another screw dislocation segment of equal length (d_2) but centered at a near-neighbor site (2 or 3). To avoid forming sharp kinks, we displaced several atomic layers near the kinks (in the xy plane perpendicular to the <111> direction) to new positions which were chosen to be the average value of atomic positions of the d_1 and d_2 segments. The total thickness or length of the simulation cell along the <111> direction was chosen to be $\sim 35a$ (with $\sim$ 18000 atoms in region I and a total number of atoms of about 43000). Finally, the structure was relaxed subject to the usual anisotropic elastic boundary conditions in region II of the computational cell. By varying the length R_k of the d_2 segment, we could investigate the stability and formation energy of different possible kink pairs. In particular, one seeks to determine the limiting value of the formation energy for an infinitely separated kink pair and also the minimum or "annihilation" distance below which the kinks become unstable after relaxation and the final configuration becomes a long straight dislocation centered on site 1 in the simulation cell.

In principle, kink pairs of different character are possible depending on whether the

segment d_2 is centered on site 2, a "hard"-core location, or on site 3, an "easy"-core location. The shortest near-neighbor distance involves site 2 and results in an "easy"-"hard"-"easy" configuration. This configuration, which lies in <110> direction on a {112} plane, was found to be unstable for all kink lengths R_k. Interestingly, however, this kink pair does not revert to the "easy"-core dislocation ground state upon relaxation. Rather a soliton structure is formed in which the d_1 and d_2 segments each have an "easy" core structure but with opposite orientations. That is, the final straight dislocation line is composed of alternating segments of the two degenerate orientations of the "easy" core structure. The instability of the "easy"-"hard"-"easy" double kink is undoubtedly related to the {110} energy barrier displayed in Fig. 4. In particular, the high formation energy of 0.24 eV/b for a "hard"-core relative to an "easy" core coupled with the shallow barrier of 0.02 eV/b which stabilizes the former probably makes it energetically favorable for any "hard" segment d_2 to migrate away and return to the "easy" site d_1.

For the remaining possible kink pair formed between sites 1 and 3, an "easy"-"easy"-"easy" configuration results. This configuration lies in a <112> direction on a {110} plane. Here the double kink is stabilized beyond a certain critical separation distance between the two kinks. This "annihilation" distance was found to be about $4b$ ($b = 2.74$ $\AA$) in bcc Mo. Our calculated formation energy per kink as a function of kink length R_k is plotted in Fig. 6. Note that two plateau regions of near constant formation energy are found. The first occurs for $4b < R_k < 14b$ where the two kinks still appear to be interacting rather strongly and the formation energy is near 0.7 eV/kink. The second region occurs for $R_k > 14b$, where the two kinks appear to become weakly coupled and the formation energy assumes an asymptotic value of 1.0 eV/kink. The total formation energy for an infinitely separated kink pair is thus inferred to be 2.0 eV.

VI. CONCLUSIONS

In summary, we have studied several important aspects of the energetics and motion of <111> screw dislocations in bcc Mo, using multi-ion MGPT interatomic potentials combined with a static atomistic simulation method. Our calculated (110) and (211) γ surfaces are qualitatively similar to those previously obtained with simplier radial-force models, but are higher in energy by as much as 50%. This demonstrates the quantitative importance of the angular-force contributions from the three- and four-ion MGPT potentials for dislocation calculations in such metals. For an applied <111>/{112} shear, our calculated Peierls stress is about 0.025μ. The related energy barriers for moving a long straight screw dislocation on the primary {110} and {112} slip planes have also been calculated. These results confirm that motion on a {110} plane is much easier (maximum energy barrier 0.26 eV/b) than on the {112} plane (maximum energy barrier 0.9 eV/b). Finally, it is found that for zero applied stress, the formation energy for a stable kink pair on a nonstraight screw dislocation approaches about 2.0 eV for kinks separated by a distance greater than $15b$, while the minimum or "annihilation" distance between two such kinks is about $4b$. In the future, we intend to extend this work to the study of kink migration and the calculation of the stress dependence of the double-kink activation energy, both in Mo and in other bcc metals such as Ta. It should also be possible to treat dislocation-dislocation interactions, including junction formation and breaking.

ACKNOWLEDGMENTS

The authors wish to thank Drs. V. Bulatov, M. S. Duesbery, V. Vitek, and S. Rao for helpful discussions. This work was performed under the auspices of the U.S. Department of Energy by the Lawrence Livermore National Laboratory under contract number W-7405-ENG-48.

REFERENCES

[1] J. W. Christian, in *Proceedings of the Second International Conference on Strength of Metals and Alloys* (ASM press, Asilomar, 1970), p. 31; B. Šestak, in *Proceedings of the Third International Symposium, Reinststoffe in Wissenschaft und Technik* (Akademie Verlag, Berlin, 1970), p. 221.

[2] V. Vitek, Crystal Lattice Defects **5**, 1 (1974) and references therein.

[3] M. Tang, G. Canova, and L. Kubin (to be published) and private communication.

[4] A. E. Carlsson, Phys. Rev. B **44**, 6590 (1991); D. G. Pettifor, Phys. Rev. Lett. **63**, 2480 (1989); M. Aoki, Phys. Rev. Lett. **71**, 3842 (1993); S. M. Foiles, Phys. Rev. B **48**, 4287 (1993); W. Xu and J. B. Adams, Surf. Sci. **301**, 371 (1994).

[5] J. A. Moriarty, Phys. Rev. B **38**, 3199 (1988).

[6] J. A. Moriarty, Phys. Rev. B **42**, 1609 (1990); J. A. Moriarty and R. Phillips, Phys. Rev. Lett. **66**, 3036 (1991).

[7] J. A. Moriarty, Phys. Rev. B **49**, 12431 (1994).

[8] W. Xu and J. A. Moriarty, Phys. Rev. B **54**, 6941 (1996).

[9] A useful set of data and subroutines implementing the present Mo interatomic potentials is available via the internet. Send e-mail requests to moriarty@sycamore.llnl.gov .

[10] J. D. Eshelby, W. T. Read, W. Shockley, Acta Met. **1**, 251 (1953); A. N. Stroh, Phil. Mag. **3**, 625 (1958); A. K. Head, Phys. Stat. Sol. **6**, 461 (1964); J. P. Hirth and J. Lothe, Phys. Stat. Sol. **15**, 487 (1966); Y. T. Chou and T. E. Mitchell, J. of Appl. Phys. **38**, 1535 (1967).

[11] V. Vitek, J. Cserti and M. S. Duesbery (to be published) and private communication.

[12] M. W. Finnis and J. E. Sinclair, Philos. Mag. A **50**, 45 (1984).

[13] M. S. Duesbery, Proc. R. Soc. London A **392**, 145 (1984).

FIGURES

FIG. 1. Cross section of the rectangular slab-shaped computational cell used in the present atomistic simulations. In region I all atomic positions are fully relaxed, while in region II atomic positions are established according to fixed or periodic boundary conditions, as described in the text.

FIG. 2. Generalized stacking fault (γ) energy surfaces for bcc Mo, in units of meV/$\AA^2$. (a) (110) plane and (b) (211) plane. The open, grey and black circles at the top on each figure represent first-, second-, and third-layer atoms, respectively. Asymmetrical twinning and anti-twinning slip along the $[\bar{1}11]$ direction on the (211) surface is indicated as "t" and "a".

FIG. 3. The <111> projection of the differential displacement (DD) maps for the mechanically stable screw dislocations in bcc Mo. (a) the ground-state "easy"-core configuration and (b) the higher-energy "hard"-core configuration. In the DD method the <111> component of the relative displacement of neighboring atoms due to the dislocation (i.e., the total relative displacement less than that in the perfect lattice) is drawn as an arrow between the corresponding atoms.

FIG. 4. Schematic representation of constrained <111> screw dislocation motion on the {110} and {112} slip planes, showing the relevant energy barriers for bcc Mo, in units of eV/b. The sites 1 and 4 represent stable "easy"-core dislocation positions, while sites 2 and 3 represent metastable "hard"-core positions, as discussed in the text.

FIG. 5. Schematic representation of kink-pair formation on a <111> screw dislocation. The quantity R_k is the separation distance between the two kinks (i.e., the kink length) and d_1 and d_2 are segments of <111> screw dislocations. The sites 1, 2, and 3 represent possible stable locations for the dislocation segments, as discussed in the text.

FIG. 6. Calculated double-kink formation energy, in units of eV/kink, for a <111> screw dislocation for bcc Mo with zero applied stress.

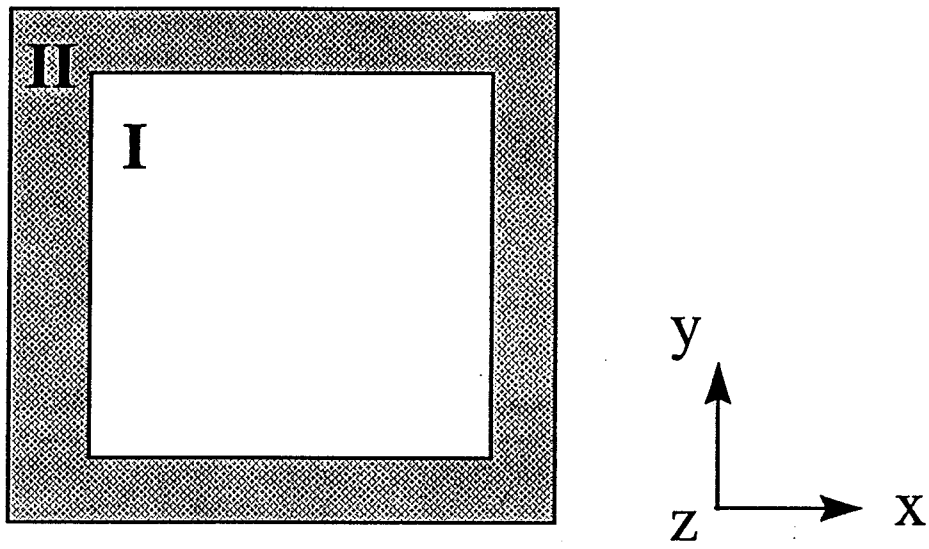

FIG. 1

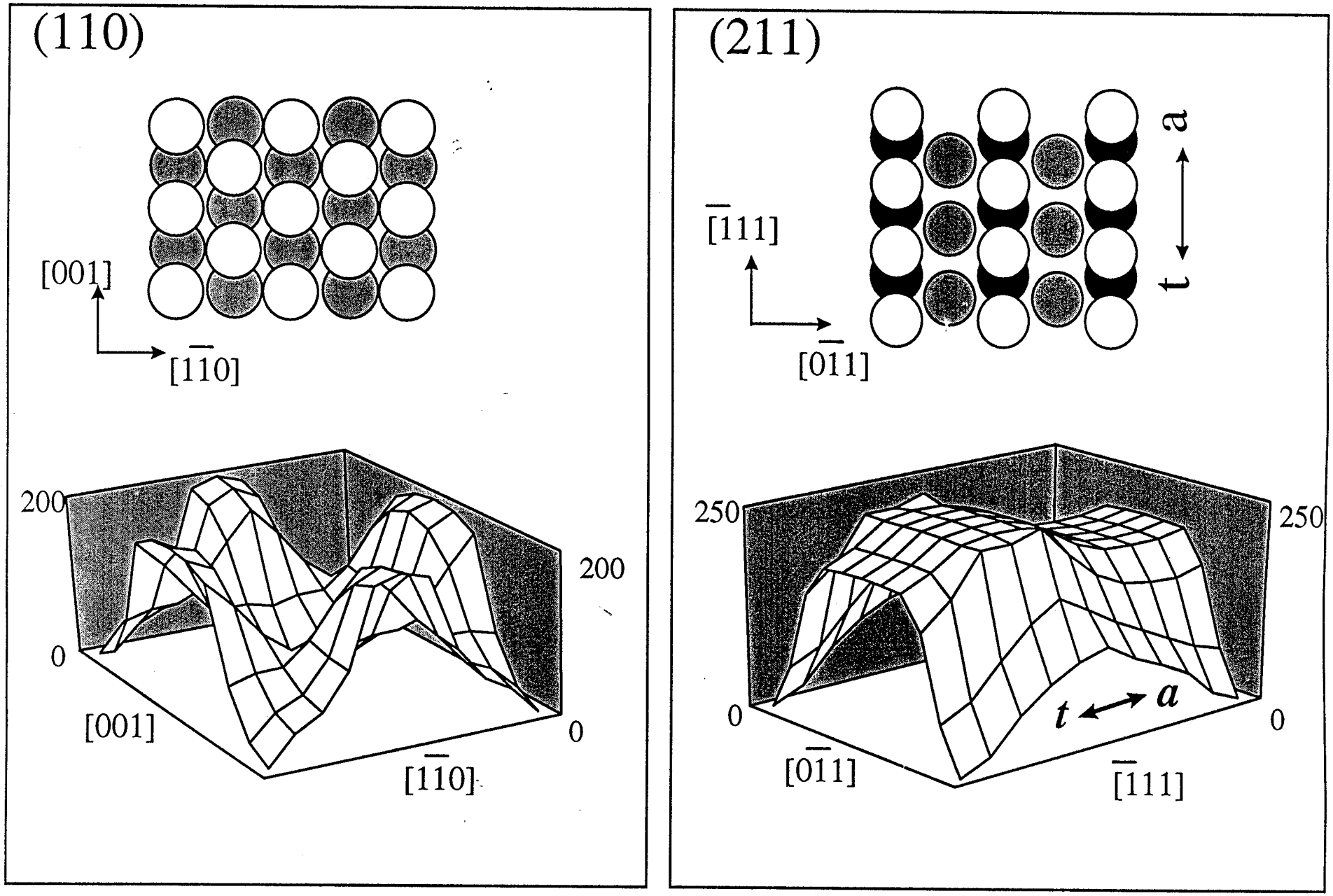
(110)
[001]
[1̄10]
200
0
[001]
[1̄10]
200
0
(211)
[1̄11]
[01̄1]
t
a
250
0
[01̄1]
t
a
[1̄11]
250
0

(a)

(b)

FIG. 2

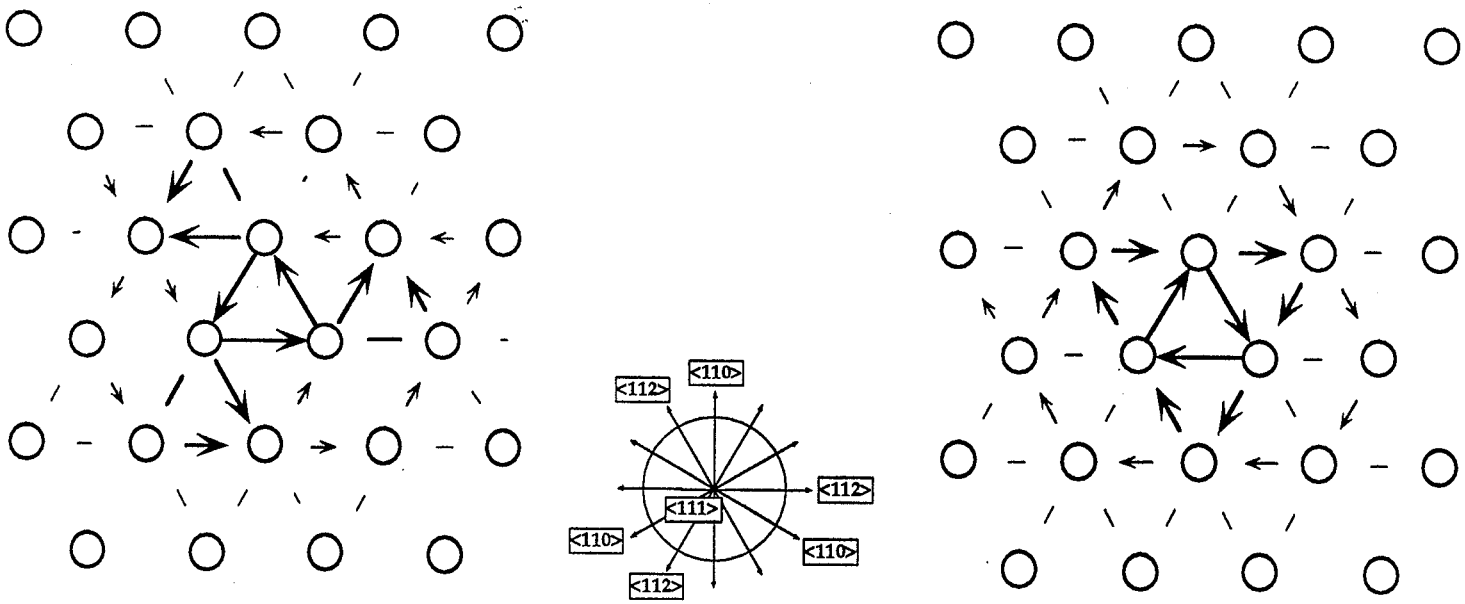

(a) (b)

FIG. 3

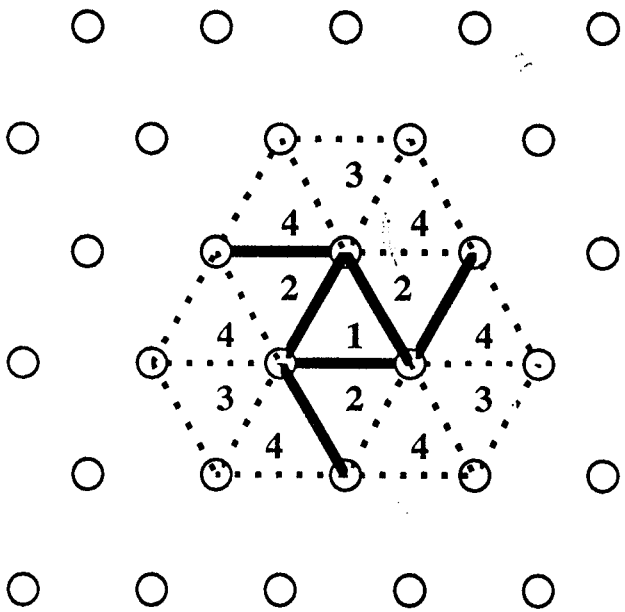
3
4
4
2
2
4
1
4
3
2
3
4
4

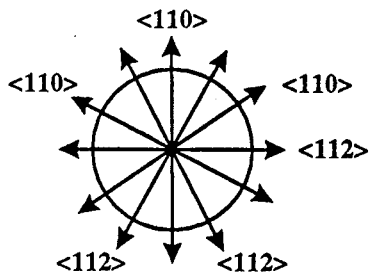
<110>
<110>
<110>
<112>
<112>
<112>

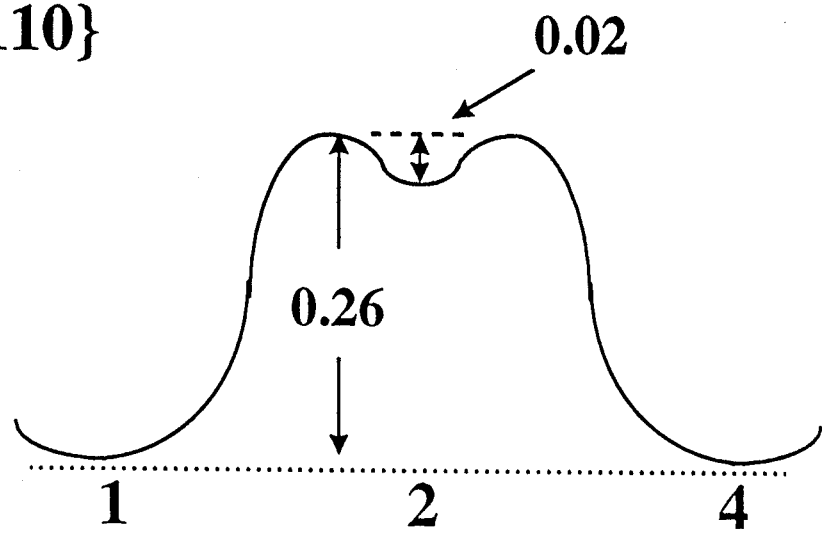
{110}
0.02
0.26
1
2
4

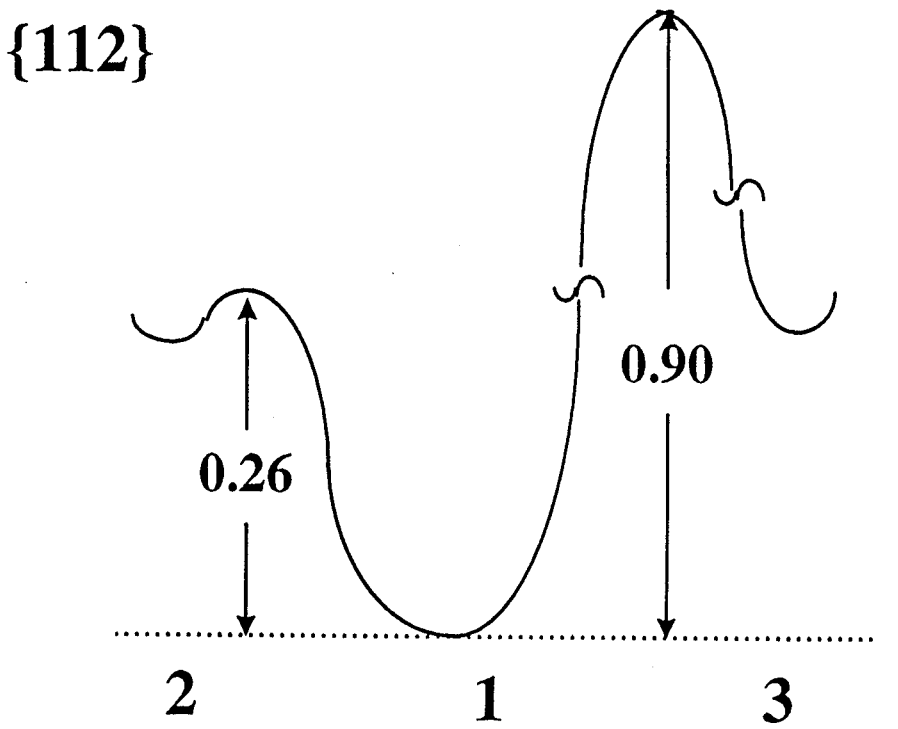
{112}
0.90
0.26
2
1
3

FIG. 4

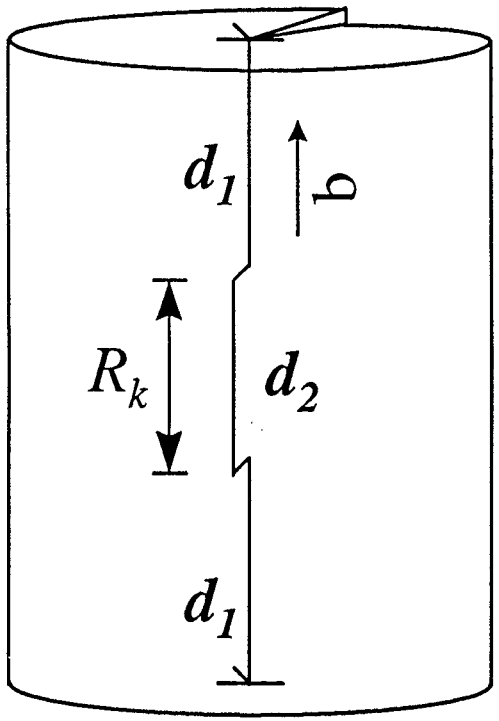

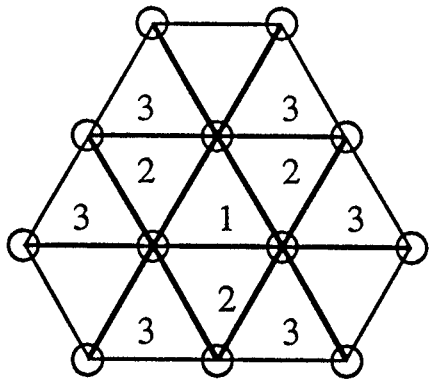

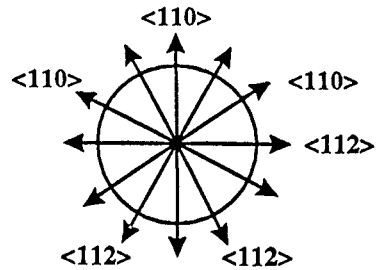

Fig. 5

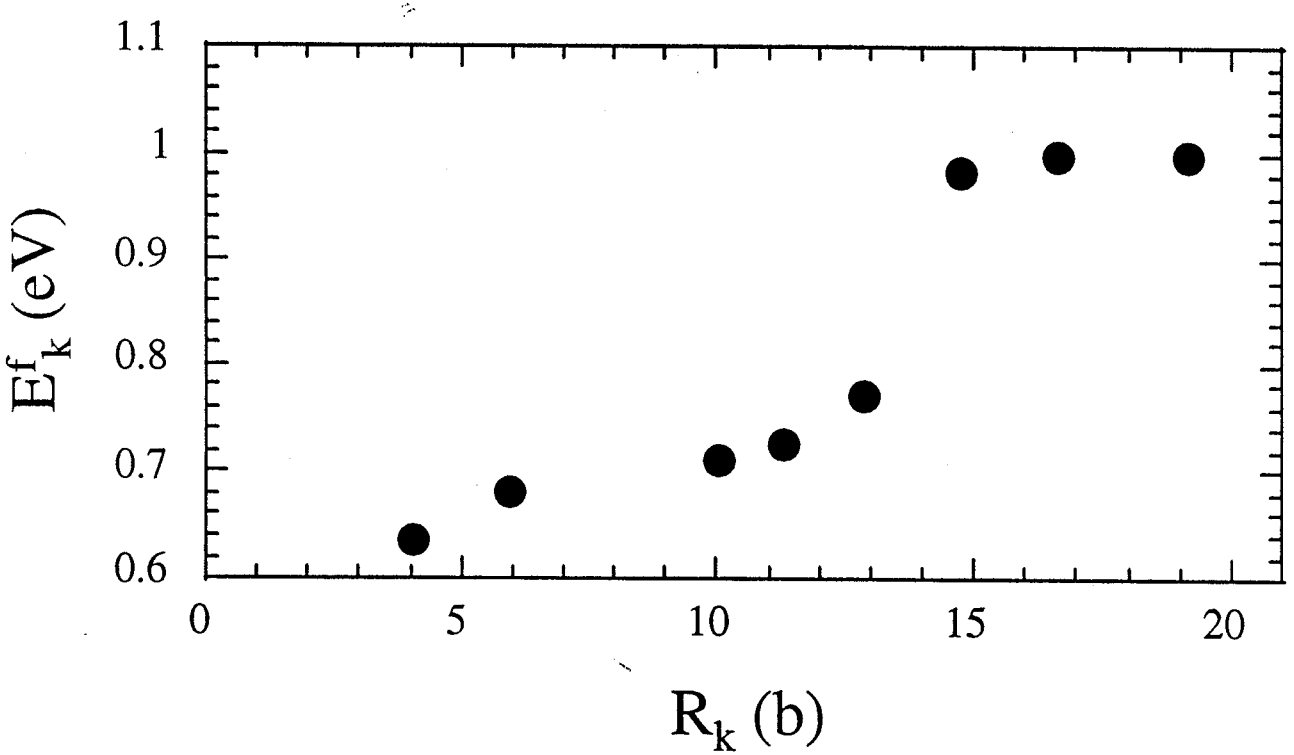

FIG. 6

Technical Information Department • Lawrence Livermore National Laboratory
University of California • Livermore, California 94551